Received: 12 August 2019 | Revised: 24 October 2019 | Accepted: 29 October 2019

DOI: 10.1002/mbo3.968

ORIGINAL ARTICLE

MicrobiologyOpen Open Access WILEY

Experimental evolution for niche breadth in bacteriophage T4 highlights the importance of structural genes

Jenny Y. Pham[1] | C. Brandon Ogbunugafor[2] | Alex N. Nguyen Ba[1] | Daniel L. Hartl[1]

[1]Department of Organismic and Evolutionary Biology, Harvard University, Cambridge, MA, USA

[2]Department of Ecology and Evolutionary Biology, Brown University, Providence, RI, USA

Correspondence
C. Brandon Ogbunugafor, Department of Ecology and Evolutionary Biology, Brown University, Providence, RI, USA.
Email: brandon_ogbunu@brown.edu

Funding information
National Science Foundation, Grant/Award Number: DGE1745303 and 1736253

Abstract

Ecologists have long studied the evolution of niche breadth, including how variability in environments can drive the evolution of specialism and generalism. This concept is of particular interest in viruses, where niche breadth evolution may explain viral disease emergence, or underlie the potential for therapeutic measures like phage therapy. Despite the significance and potential applications of virus–host interactions, the genetic determinants of niche breadth evolution remain underexplored in many bacteriophages. In this study, we present the results of an evolution experiment with a model bacteriophage system, *Escherichia virus T4*, in several host environments: exposure to *Escherichia coli* C, exposure to *E. coli* K-12, and exposure to both *E. coli* C and *E. coli* K-12. This experimental framework allowed us to investigate the phenotypic and molecular manifestations of niche breadth evolution. First, we show that selection on different hosts led to measurable changes in phage productivity in all experimental populations. Second, whole—genome sequencing of experimental populations revealed signatures of selection. Finally, clear and consistent patterns emerged across the host environments, especially the presence of new mutations in phage structural genes—genes encoding proteins that provide morphological and biophysical integrity to a virus. A comparison of mutations found across functional gene categories revealed that structural genes acquired significantly more mutations than other categories. Our findings suggest that structural genes are central determinants in bacteriophage niche breadth.

KEYWORDS

bacteriophage, experimental evolution, niche breadth, structural genes, trade-off

1 | INTRODUCTION

Experimental evolution has served an important role in the study of niche breadth in microbes (Kassen, 2002). Many of these studies have focused on virus systems and experimental exposure to different (or new) hosts, as the type, range, and availability of hosts present in the environment is an important source of selection pressure (Cooper & Scott, 2001; Crill, Wichman, & Bull, 2000; Duffy, Burch, & Turner, 2007; Enav, Kirzner, Lindell, Mandel-Gutfreund, & Béjà, 2018; Kutnjak, Elena, & Ravnikar, 2017; Morley, Mendiola, & Turner, 2015; Novella et al., 1995). This and other experimental work in this realm has provided varying levels of support for the trade-off hypothesis—that the ability to broadly exploit hosts (generalism) comes at the cost of the ability to exploit any

single niche (specialism) (Bedhomme, Lafforgue, & Elena, 2012; Novella, Hershey, Escarmis, Domingo, & Holland, 1999; Turner & Elena, 2000). In particular, there have been relatively few rigorous treatments of the evolutionary genomics of niche breadth expansion, where the genetic determinants of niche breadth are resolved with functional inferences drawn between mutations and phenotypes. Such studies continue to have practical relevance for questions about the phenotypic manifestations of niche breadth evolution, whether trade-offs arise as a consequence of adaptation, and about the molecular signatures of such evolution.

In this study, we sought to characterize the phenotypic and molecular changes associated with niche breadth evolution in a model bacteriophage. We employ *Escherichia virus T4* as a system for experimental evolution. T4 is of particular interest because it is among the most well-studied and fully characterized viruses. T4 is also surprisingly complex, with a genome ~170 kb in size and a gene density four times greater than that of herpes viruses and twice that of *Escherichia coli*. Of its 300 genes, approximately 160 have been functionally characterized (Miller et al., 2003), which provides the opportunity to resolve molecular mechanisms responsible for niche breadth evolution. We evolved T4 for 50 generations in one of three host environments: (a) *E. coli* C, (b) *E. coli* K-12, and (c) daily alternation of *E. coli* C and *E. coli* K-12 (Figure 1).

Selection on either *E. coli* C or *E. coli* K-12 mimics a constant environment, which is predicted to drive the evolution of specialists; whereas selection on the alternating hosts mimics a temporally variable environment, which is predicted to drive the evolution of generalists (Turner & Elena, 2000). Our results reveal the complexity of niche breadth evolution, with some populations demonstrating properties of a trade-off, others less so. The genomic data reflected patterns across evolutionary histories: new mutations were overrepresented in genes that encode structural virion proteins. Notably, this pattern implies that structural genes—and in particular, those that function in host recognition, infection, and stability—are important in niche breadth evolution, regardless of conditions that promoted a particular ecological strategy (specialism or generalism). We discuss these findings in detail, and reflect on their implications for general viral ecology, and for the various arenas where bacteriophage niche breadth has practical utility—in disease emergence, public health surveillance, and efforts to engineer bacteriophage for therapeutic purposes.

2 | MATERIALS AND METHODS

2.1 | T4 and bacterial strains

This study used *Escherichia virus T4* (American Type Culture Collection [ATCC] #11303-B4) and three wild-type bacterial hosts: *E. coli* B (ATTC #11303), *E. coli* C (Coli Genetic Stock Center 3,121), and *E. coli* K-12 (Coli Genetic Stock Center 4,401). T4 infection of *E. coli* K-12 has been well documented (Yu & Mizushima, 1982), but not *E. coli* C, which is a strain normally used for the propagation of *Escherichia virus phiX174* (Wichman, Millstein, & Bull, 2005). *E. coli* B is the strain that has been historically used for the propagation of T4 (Demerec & Fano, 1944) and currently recommended by the ATCC for T4 propagation. Bacteria were stored as 25% glycerol stocks at −80°C; isolated bacterial colonies were obtained by streaking stocks onto lysogeny broth (LB) agar (Miller formula) petri dishes (BD, VWR International). All assays and serial passaging utilized liquid bacterial cultures which were prepared daily; single colonies were inoculated into glass culture tubes containing 5 ml of LB broth and incubated overnight at approximately 180 RPM (C1 Platform Shaker, New Brunswick Scientific) and 37°C. The T4 ancestral clone used to initiate experimentally evolved lines was isolated by plaque purification on LB agar petri dishes containing overlays comprised of 10 µl serially diluted phage lysate, 30 µl (~10^8 colony-forming units [CFU]/ml) bacterial host culture, 270 µl LB broth, and 4 ml LB soft agar (7.5 g/L agar). Following overnight incubation at 37°C, a single well-formed plaque was isolated, saturated with 500 µl LB broth, treated with 4% chloroform (VWR Life Science), and stored at 4°C.

2.2 | Experimental evolution of T4

To initiate the experimental evolution, the T4 ancestral clone was used to seed 15 populations. Three sets of five parallel populations were evolved in one of three host environments: (a) *E. coli* C, (b) *E. coli* K-12, and (c) a daily alternating pattern of *E. coli* C and *E. coli* K-12 (Figure 1). The initial passage was perf(ormed in LB agar petri dishes containing overlays comprised of the T4 ancestral clone, appropriate bacterial host, 270 µl LB broth, and 4 ml LB soft agar, with initial infection occurring at MOI = 0.001 (volumes for T4 and bacteria were variable due to differences in host growth). Following overnight incubation at 37°C, phage lysates were collected, treated with 4% chloroform, centrifuged at 7,500 rpm and 4°C for 20 min (J6-MI, Beckman Coulter), and sterilized using 0.2 µm syringe filters (Pall Life Sciences). 500 µl of each phage lysate was saved for storage at 4°C. These steps ensured that all bacteria were removed from phage lysates prior to usage for subsequent passages. Passages following the initial infection were plated as overlays on LB agar petri dishes, which contained 10 µl of phage lysate, 30 µl bacterial host culture, 270 µl LB broth, and 4 ml of LB soft agar, followed by overnight incubation at 37°C. Lysates generated over the course of the experimental evolution were collected, purified, and stored in the same manner as the initial lysate. In all passages, phage populations were propagated with hosts derived from newly prepared overnight bacterial cultures (no possibility for coevolution). To prevent cross-contamination between evolutionary histories, each set of parallel populations was confined to separate laboratory rooms, and lysate supernatants were collected and purified using only materials (i.e., micropipettes and plastics) contained to the same room. Serial passaging was performed for 20 days, which is assumed to be equivalent to ~ 50 generations of T4 growth (we elaborate on generation time in the Appendix A).

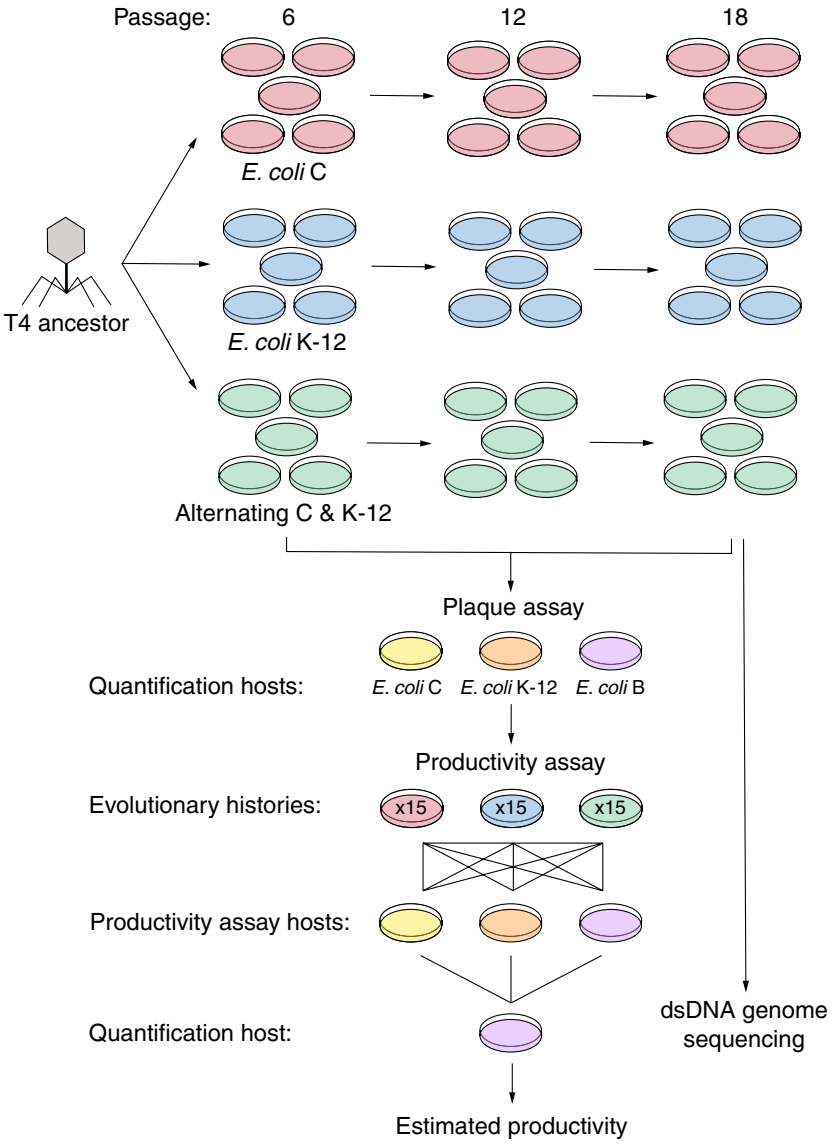

FIGURE 1 *Experimental evolution schematic*. 15 populations were seeded with a previously isolated T4 ancestral clone and split into three evolutionary histories with different host environments: Five populations were exposed to *Escherichia coli* C; another five were exposed to *E. coli* K-12; and the last five were exposed to *E. coli* C and K-12 in daily alternation. Serial passaging occurred for 20 days, which is equivalent to approximately 50 generations. Plaque assays on the original host *E. coli* B and the selection host *E. coli* C and/or K-12 were performed for quantification of evolved phage samples on passages 6, 12, and 18. To measure productivity, assays on *E. coli* C, K-12, and B were performed for the same evolved samples. Following the productivity assay, samples were quantified using *E. coli* B, which generated the final estimate of productivity ($\log_{10}$ titer [pfu/ml]). Sequencing was performed on the complete genomes of the T4 ancestor and 15 evolved populations at passage 18

2.3 | Phage quantification

Quantification was accomplished using plaque assays in which 4 µl of 10-fold serial dilutions of phage lysates were spotted on LB agar petri dishes containing overlays comprised of 30 µl bacterial host culture, 270 µl LB broth, and 4 ml LB soft agar. Petri dishes were incubated overnight at 37°C, with plaque visualization and counting occurring the following day. Quantified phage samples were expressed as PFU/ml; each plaque was assumed to have originated from a single infecting phage particle; thus, one plaque was equivalent to one PFU. Throughout the experiment, *E. coli* B was used for quantification because it is a consistent and highly permissive host. Following the experimental evolution, three replicate plaque assays (n = 3) were performed on the 15 populations at passage 6, 12, and 18, using both the selection host/hosts and the original host, to confirm that *E. coli* B remained a more sensitive host. This yielded 315 data points ([5 populations × 2 single host histories × 3 time points × 2 quantification hosts × 3 replications] + [5 populations × 1 alternating host history × 3 time points × 3 quantification hosts × 3 replications]). Replicate titers were $\log_{10}$-transformed and compared for differences due to quantification host using unpaired t tests; each comparison was comprised of 30 measurements because titers were pooled by evolutionary history. In total, 12 comparisons were made using GraphPad Prism v. 7.0b (GraphPad Software, La Jolla California USA).

2.4 | Productivity assays

Productivity assays were performed to measure phage titers produced on three hosts: *E. coli* C, *E. coli* K-12, and *E. coli* B. Following the experimental evolution, assays were performed on the 15 populations at passage 6, 12, and 18. Productivity assays were standardized by infection of phage samples and bacteria at MOI = 0.001 and measured total number of progeny produced. Each assay was performed on LB agar petri dishes containing overlays comprised of 10 µl diluted phage lysate, 1 µl diluted bacterial host, 270 µl LB broth, and 4 ml LB soft agar. Following overnight incubation at 37°C,

phage lysates were collected and purified using the same methods as those applied to the serial passages. Lastly, phage lysates were quantified for titer using plaque assays (as described above) and *E. coli* B as the quantification host.

In total, three replicate productivity assays ($n = 3$) were performed, which resulted in 405 titer measurements (5 populations × 3 evolutionary histories × 3 time points × 3 assay hosts × 3 replications). Titer measurements used in the linear mixed effects model were $\log_{10}$-transformed to improve normality. The model was generated using the lmer function of the lme4 R package (Bates, Mächler, Bolker, & Walker, 2015). The initial model included replication as an additional random factor; however, this parameter was dropped because the variance estimate was extremely small (*variance* = 0.00142) when compared with the variance of the residual error (*variance* = 0.11195). To confirm goodness of fit and ensure that model assumptions were met, model residuals were visually inspected (Zuur, Ieno, & Elphick, 2010). Plotted residuals were normally distributed and revealed no concerning patterns of heterogeneity in variances. The analysis of variance table was calculated using the ANOVA function of the car R package, which performs Wald chi-square tests for linear mixed effects models (Fox & Weisberg, 2011). Follow-up analysis was performed using the contrast function of the lsmeans R package to obtain pairwise comparisons among LS means (Lenth, 2016). *P* values generated from this analysis were adjusted using the Holm method, which is designed to give strong control of the family-wise error rate while retaining more power than the Bonferroni correction. The results of this analysis are available in Appendix B.

Additional productivity assays ($n = 3$) were performed for the T4 ancestor in order to gauge baseline titer on the three assay hosts. These data were excluded from the linear model and analyzed using one-way ANOVA followed by Tukey's HSD test. Titer measurements of the ancestor were necessarily excluded from the linear model because by definition, the ancestor did not have an evolutionary history nor was it serially passaged. All above analyses were performed in R v. 3.3.3 (R Development Core Team, 2017).

2.5 | Phage DNA extraction

Phage lysates were newly generated from the original evolved phage samples for library preparation (grown on *E. coli B*, a highly permissive host). This step was performed for two reasons: (a) to preserve the original 500 µl generated directly from the serial passaging, and 2) phage DNA extraction protocols generally require at least 1 ml of high titer (>10^9) phage lysate to generate high yield, clean DNA. Lysates were created from evolved samples at passage 18, the final time point that was assayed for productivity (Figure 1). These were plated as overlays on LB agar petri dishes, which contained 10 µl of evolved phage sample, 30 µl bacterial host culture, 270 µl LB broth, and 4 ml of LB soft agar. Following overnight incubation at 37°C, lysates were collected and purified in the same manner as with the serial passaging.

1 ml of each lysate was first treated with 12.5 µl 1M $MgCl_2$ (VWR Life Science), 0.4 µl DNase 1 (2000 U/ml) (New England Biolabs), and 10 µl RNase A (10 mg/ml) (Thermo Fisher Scientific). Following brief vortexing and room temperature (RT) incubation for 30 min, the following reagents were added: 40 µl of 0.5 M EDTA (Corning), 2.5 µl Proteinase K (20 mg/ml) (Thermo Fisher Scientific), and 25 µl 10% SDS (VWR Life Science). The mixture was vortexed vigorously and incubated at 55°C for 60 min, with additional mixing occurring twice at 20 min intervals. Phage DNA was extracted using an equal amount of phenol:chloroform:isoamyl alcohol (25:24:1) (VWR Life Science) to lysate. Following inversion mixing and centrifugation at RT for 5 min at 13K, the aqueous layer was removed, and two further extractions were performed in the same manner. Phage DNA was precipitated by addition of 1 ml 90% ethanol (Pharmco) and 50 µl 3M sodium acetate (Corning). Following incubation on ice for 5 min, DNA was gently mixed and centrifuged at room temperature for 10 min at 13K. The DNA pellet was washed with 500 µl 70% ethanol and centrifuged at RT for 10 min at 13K. The ethanol was decanted, and the pellet was air-dried for ~ 20 min. DNA was reconstituted in 50 µl TE buffer (Invitrogen) and checked for purity and concentration with Nanodrop 2000 (Thermo Scientific).

2.6 | Library preparation and sequencing

Library preparation was executed according to previously published protocols (Baym et al., 2015). Minor protocol modifications were made and are thus noted. In module 1, DNA was standardized with Qubit dsDNA HS Assay Kit (Thermo Fisher Scientific). In module 4, DNA size selection was performed twice (rather than once). First, 0.55 × magnetic beads were added to genomic DNA to remove large (> 600 bp) fragments. Following incubation at RT for 5 min, the tubes were placed on a magnetic stand, and the supernatant was removed and transferred to new PCR strip tubes. In the second size selection, 0.3 × magnetic beads were added to the supernatant to bind DNA fragments of desired length (~250–600 bp). Following incubation at RT for 5 min, tubes were placed on a magnetic stand, and the supernatant was removed and discarded. The beads were washed once with 200 µl 80% ethanol, allowed to air-dry for ~ 20 min, and resuspended in 30 µl TE buffer. In module 4, DNA was quantified using Qubit dsDNA HS Assay Kit; libraries were pooled at 5 ng per sample, and fragment size was assessed with Agilent 4,200 TapeStation System. The final pooled library sample was sent to Bauer Core Facility (Harvard University, Cambridge, MA) for QPCR quality control and sequencing using Illumina NextSeq 500 Mid Cycle (2 150 bp).

2.7 | Analysis of sequence data

Demultiplexed reads were trimmed for Nextera adapter sequences using Trimmomatic with default settings (Bolger, Lohse, & Usadel, 2014). The reads were aligned to the T4 reference genome (RefSeq accession no. GCF_000836945.1) using Breseq v. 0.31.1 (Deatherage & Barrick, 2014). For populations, the polymorphism mode was enabled, and no junction predictions were made. Typical coverage depth was over 1,000 × for most positions in the genome

with over 95% of the reads mapping. The ancestral clone sample was replicated in the library preparation stage to account for sequencing errors and potential variation between the reference genome and the ancestral clone. Following sequencing, mutations were called separately for the two ancestral clone samples; these replicates revealed complete agreement between the called mutations. The ancestral mutations were subsequently filtered from all evolved populations in order to account for mutations that were present in the T4 ancestor but absent in the reference genome. The default Breseq configuration requires a mutation to be found in at least 5% of the reads; hence, only SNPs present in the populations at 5% or greater were considered. All polymorphisms and their frequencies are available in Appendix B.

In the genomic analysis, sequencing error bias presented barriers for the determination of polymorphisms. To remedy this, mutations with consistent statistical evidence of strand bias were removed in circumstances where the mutation would not be called when considering information from one strand versus the other. Specifically, mutations were filtered due to strand bias in cases where there existed at least 5% difference between the forward and reverse strand (preventing cases where a mutation is found in 4.9% on one strand, and 5.1% on the other one, but filtering out cases where a mutation is found in 1% in one strand, but 6% on the other). xNPs (multiple adjacent nucleotide polymorphisms) similarly presented challenges to the NGS analysis pipeline, as it did not recognize sequential mutations as one mutational event, but rather multiple events. This issue manifests in the context of calling amino acid changes, that is, when two adjacent mutations occur within one codon, two different amino acid changes are detected for each mutation, rather than one amino acid change which incorporates both nucleotide substitutions. In these cases, reads were visualized to ensure all putative xNPs occurred within the same read (as opposed to a situation where mutations occurred separately in different reads) to validate the presence of xNPs. The amino acid calls were subsequently manually modified to reflect the true amino acid change. A similar issue occurred with indels; each indel was reported as multiple mutational events rather than one. These situations were resolved in the same manner as xNPs. A final issue occurred in which a fixed ancestral mutation was detected as a new polymorphism, when it decreased in frequency due to a new mutation. This new mutation was not detected because the nucleotide substitution was coincidentally the same base as that of the reference sequence used for alignment. This error was confirmed and manually corrected by visualizing reads containing the relevant position. A list of corrected positions is available in Appendix B.

2.8 | Analysis of mutation distribution

The number of nucleotide sites occupied by each functional category was determined using previous gene designations (Miller et al., 2003) and the T4 genomic sequence associated with that study (Genbank accession no. AF158101.6). From this, the mutation rate (number of mutations per nucleotide site) of each functional gene category was calculated for the 15 evolved populations. All polymorphisms detected at or above 5% were considered for this analysis. A SRH nonparametric two-way ANOVA (Sokal & Rohlf, 2011) was performed to test the influence of factors evolutionary history, functional gene category, and their interactions on rate of mutation. This analysis was first performed for all mutations and then repeated separately for synonymous and nonsynonymous mutations. The analyses were executed using the Scheirer–Ray–Hare function of the rcompanion R package (Mangiafico, 2018). Follow-up analysis of pairwise comparisons was performed using Dunn's test, which was executed using the dunnTest function of the FSA R package (Ogle, 2018). *P* values generated from the pairwise comparisons were adjusted using the Holm method. All above analyses were performed in R v. 3.3.3 (R Development Core Team, 2017).

3 | RESULTS

3.1 | The baseline productivity of the T4 ancestral clone differs according to host strain

Before discussing the results corresponding to the state of phage populations postexperimental evolution, we first examined the baseline productivity of bacteriophage T4 across the various hosts (*E. coli* C, *E. coli* K-12, and *E. coli* B) used in the experimental evolution. The purpose of this analysis was to address questions about how ancestral populations performed across backgrounds, prior to the evolution experiment. Phage productivity was chosen as an estimate for gauging performance on a particular host because it represents the number of infectious progeny produced (per infected bacterium or per parent virion) from an infection (Abedon, Herschler, & Stopar, 2001; Kerr, Neuhauser, Bohannan, & Dean, 2006). The ancestral clone displayed differing levels of productivity on each host strain, which was expressed as mean titer ($\log_{10}$ plaque-forming units [PFU]/ml). Productivity was predictably highest on the ancestral host *E. coli* B (10.37 $\log_{10}$ PFU with 0.14 standard deviation [*SD*]), slightly lower on *E. coli* K-12 (9.77 $\log_{10}$ PFU, 0.06 *SD*), and lowest on *E. coli* C (6.10 $\log_{10}$ PFU, 0.20 *SD*) (Figure 2a). Analysis of these data using one-way ANOVA followed by Tukey's Honest Significant Differences (HSD) test indicated that productivity differences were significant ($p < .01$). Notably, T4 productivity was slightly different but high on *E. coli* K-12 and B, while productivity on *E. coli* C was several orders of magnitude (on the order of 10^4) lower than the others.

3.2 | After evolution, *E. coli* B remained the most sensitive phage quantification host

Following experimental evolution, samples required quantification of phage titer prior to being assayed for productivity. *E. coli* B is commonly

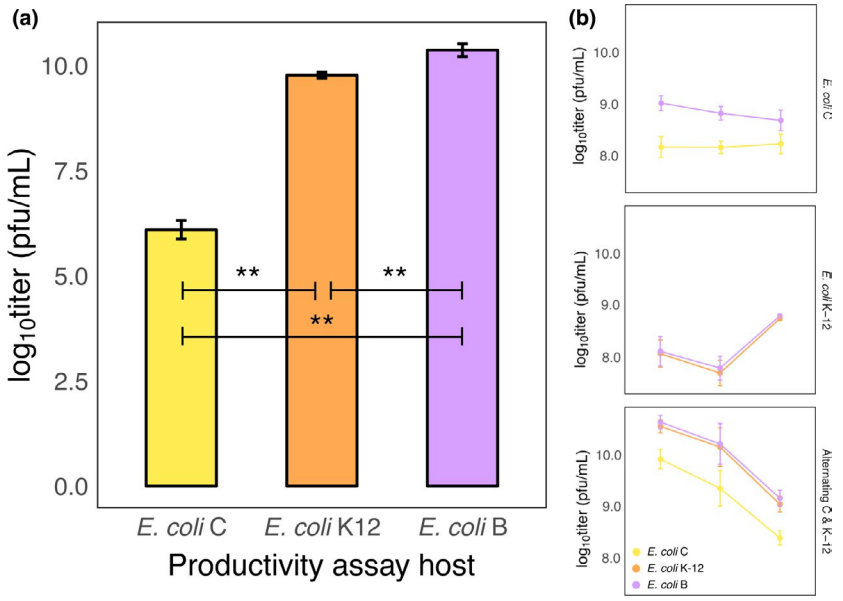

FIGURE 2 *Productivity of T4 clones*. (a) Ancestral clones (before evolution). Productivity of the T4 ancestral clone was measured on the experimental evolution hosts, *Escherichia coli* C and K-12, and on the original host, *E. coli* B. Each bar represents mean productivity ($\log_{10}$ titer [pfu/ml]) measured over three replicate assays, and error bars indicate 95% confidence limits. Analysis using one-way ANOVA followed by Tukey's HSD test indicated that all comparisons of mean titer were significant ($p < .01$). (b) Evolved clones. The 15 populations were quantified for phage titer on the original host *E. coli* B and the selection host(s) *E. coli* C and/or K-12 at passages 6, 12, 18. Plaque assays for each population were performed with threefold replication. Panels indicate one of three evolutionary histories, and each point represents grand mean titer ($\log_{10}$ PFU/ml) of the five populations within each evolutionary history; error bars indicate 95% confidence limits of the grand mean. A series of *t* tests comparing titers pooled by evolutionary history indicated that all comparisons involving *E. coli* C and B yielded significant differences (with the higher titer estimate occurring on *E. coli* B), and all comparisons involving *E. coli* K-12 and B yielded no significant differences (see main text and Table 1)

used for T4 quantification because it is a consistent and highly permissive host. We anticipated a potential problem because selection on the other hosts (*E. coli* C and/or *E. coli* K-12) could lead to correlated antagonistic changes (*i.e.*, reduced infectivity) on the original host.

Plaque assays were performed on the 15 evolved populations at three time points (passage 6, 12, and 18) to investigate whether *E. coli* B remained a more sensitive quantification host than the selected host(s) (*E. coli* C and/or *E. coli* K-12). Results from these plaque assays indicated that phage titer measurements, expressed as $\log_{10}$ PFU/mL, on *E. coli* B were either equivalent or greater than those on the selected host(s) (Figure 2b). Specifically, the grand mean titer for *E. coli* C evolved populations was higher on *E. coli* B than that on *E. coli* C for all time points, indicating that *E. coli* B was a more sensitive quantification host. The grand mean titer for *E. coli* K-12 evolved populations was equivalent whether quantified on *E. coli* B or K-12 for all time points, indicating that these two strains were equally sensitive as quantification hosts. The grand mean titer for evolved populations with alternating hosts recapitulated the results of the single host evolved populations. For all time points, *E. coli* B provided equivalent titer measurements when compared with *E. coli* K-12 and more sensitive measurements when compared with *E. coli* C. Furthermore, a series of *t* tests conducted on titer measurements pooled by evolutionary history indicated that all comparisons involving *E. coli* C and *E. coli* B as quantification hosts yielded significant differences (with the higher titer estimate occurring on *E. coli* B) whereas all comparisons involving *E. coli* K-12 and *E. coli* B yielded no significant differences (Table 1). These results confirm that, despite selection on different hosts, *E. coli* B remained the most highly permissive host and thus was used for quantification of phage titer throughout this study.

TABLE 1 *p* Values[a] of *t* tests comparing $\log_{10}$ titer of T4 populations after plaque quantification on the evolved host(s) versus *Escherichia coli* B

		Passage		
Evolved host	Comparison	6	12	18
E. coli C	C vs. B	<0.0001	<0.0001	<0.0001
E. coli K–12	K–12 vs. B	0.6603	0.3759	0.0424
Alternating	C vs. B	<0.0001	<0.0001	<0.0001
	K–12 vs. B	0.2034	0.6674	0.1273

[a]The Bonferroni correction was applied to the critical value ($\alpha = 0.004$) to adjust for multiple comparisons.

3.3 | Niche breadth evolution resulted in changes in phage productivity over time

After 20 days of host selection, the 15 evolved populations (5 3 replicates) were assayed for productivity on three hosts (*E. coli* C, K-12, and B) at three equidistant time points (passage 6, 12, and 18). We measured phage productivity at three time points and

across histories and assay hosts, relative to the productivity of the ancestor. This experiment yielded a total of 405 productivity measurements (including $n = 3$ replicate assays). Mixed effects linear modeling fit by restricted maximum likelihood was used to test for the effects of experimental treatments—evolutionary history, assay host, and number of passages—on phage productivity. Evolutionary history, assay host, number of passages, and their interactions were specified as fixed factors, and population nested within history was specified as a random factor. We used the model to generate predicted least squared (LS) means for productivity at each level of evolutionary history, assay host, and number of passages (Figure 3). Due to the presence of interactions, a type III analysis of deviance table was calculated to determine the significance of each fixed parameter and their interactions in explaining variation in phage productivity (Table 2). This analysis revealed that all fixed factors and their interactions had a significant effect on productivity.

In addition, we performed pairwise comparisons on predicted LS means for productivity between evolutionary histories for each level of assay host and number of passages (see Figure 3 for a graphical representation and Appendix B for numerical estimates). Focusing on the final time point (passage 18) and assay host *E. coli* C, all contrasts of predicted means for phage productivity between evolutionary histories were significant ($p \leq .001$), indicating that by passage 18, evolutionary history led to different outcomes of productivity on *E. coli* C. Predicted productivity was highest for populations evolved on *E. coli* C (*LS mean* = 7.14, *95% CI* = [6.93; 7.35]), lower for populations evolved on alternating hosts (*LS* mean = 6.63, *95% CI* = [6.41; 6.84]), and lowest for populations evolved on *E. coli* K-12 (*LS mean* = 5.76, *95% CI* = [5.55; 5.97]). At passage 18 and assay host *E. coli* K-12, all contrasts of predicted means for phage productivity between evolutionary histories were not significant ($p > .1$), indicating that evolutionary history had the same effect on productivity on *E. coli* K-12 at this time point. Furthermore, all predicted productivities on *E. coli* K-12 were lower than that of the ancestor (*E. coli* C *LS mean* = 8.93, *95% CI* = [8.72; 9.14]; *E. coli* K-12 *LS mean* = 9.00, *95% CI* = [8.79; 9.21]; alternating host *LS mean* = 8.69, *95% CI* = [8.48; 8.90]). At passage 18 and assay host *E. coli* B, contrasts of predicted means for phage productivity between the alternating host history and the *E. coli* C and *E. coli* K-12 histories were significant ($p < .01$) while the difference between the predicted means of the two single host histories was not significant ($p = .60$). Interestingly, all predicted productivities on *E. coli* B were also lower than that of the ancestor, with the lowest productivity belonging to the alternating history (*E. coli* C *LS mean* = 9.14, *95% CI* = [8.92; 9.35]; *E. coli* K-12 *LS mean* = 9.21, *95% CI* = [9.00; 9.43]; alternating host *LS mean* = 8.68, *95% CI* = [8.47; 8.89]).

3.4 | Genetic signatures are suggestive of positive selection in evolved populations

Following the experimental evolution, the genomes of the 15 evolved populations at passage 18 were sequenced to analyze

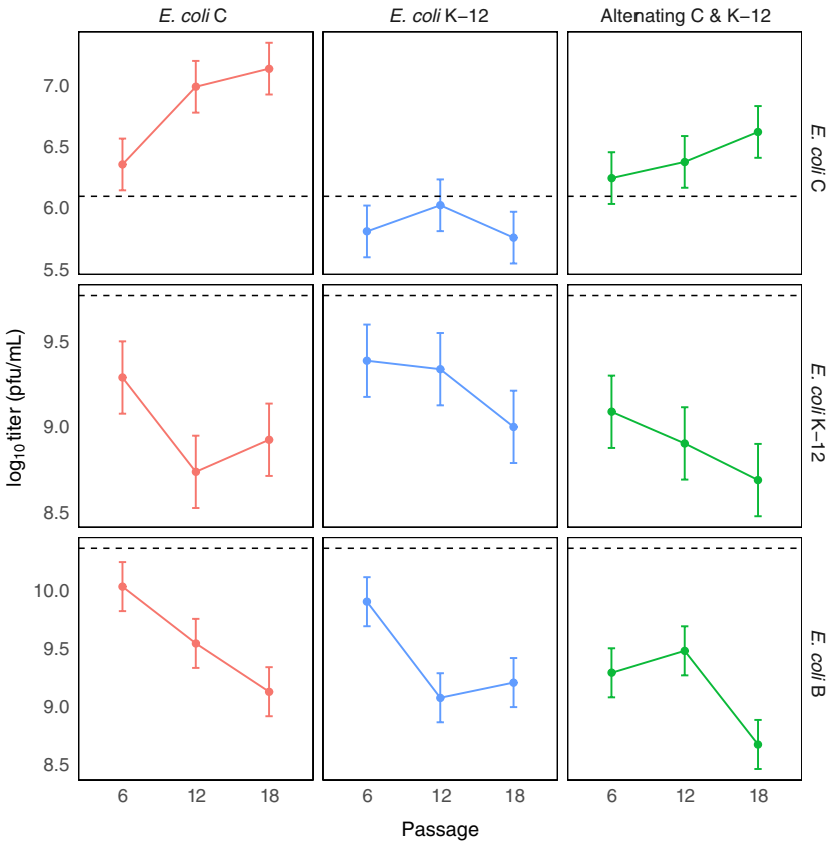

FIGURE 3 *Model predictions of mean productivity*. Predicted LS means for productivity at each level of evolutionary history, assay host, and number of passages (estimates were not provided for individual populations because population was specified as a random factor). Horizontal rows denote the assay host, and vertical columns and colors denote evolutionary history. Each point represents LS mean productivity ($\log_{10}$ titer [pfu/ml]), and error bars indicate 95% confidence limits. Dashed black lines indicate the productivity of the T4 ancestor on a particular assay host to provide a frame of reference

TABLE 2 Analysis of deviance table for a mixed effects linear model testing the effect of each fixed parameter and their interactions on productivity ($\log_{10}$ titer) of evolved T4 populations

Fixed effects	Chi-sq	*df*	Pr(>chi-sq)
Evolutionary history	14.898	2	0.0005
Assay host	1,004.209	2	<0.0001
Number of passages	45.812	2	<0.0001
History × assay	45.366	4	<0.0001
History × passages	28.224	4	<0.0001
Assay × passages	115.056	4	<0.0001
History × assay × passages	74.234	8	<0.0001

[a]Type III Wald chi-sq test.

mutations and their frequencies. The small genome size of T4 coupled with current sequencing technology yielded over 1,000 × coverage depth for most positions in the genome, with over 95% of the reads mapping unambiguously to the T4 reference genome; this enabled the reliable detection of polymorphisms occurring at 5% frequency or greater. A total of 174 mutations occurred across 145 loci, with a range of 3–30 mutations per population and 77.6% occurring as unique to a particular population (for a graphical representation see Figure 4, and for a complete list see Appendix B). Of the total number of mutations, 2.8% occurred in intergenic regions; 6.9% were indels; 82.2% were single nucleotide polymorphisms (SNPs); and 8.1% were multi-nucleotide polymorphisms (xNPs). All xNPs were nonsynonymous, and among them, 14.7% were synonymous, and 85.3% were nonsynonymous. Of the total number of detected SNPs, we observed a dN/dS ratio of 5.8. If observed indels and xNPs are also classified as nonsynonymous (each instance is conservatively counted as one nonsynonymous mutation despite causing more than one amino acid change in most cases), this ratio increases to 7.0 (Figure 5 and Table 3). Across evolutionary histories, we observed that few mutations reached fixation, with the preponderance of those being nonsynonymous mutations. These signatures indicate that positive selection shaped phenotypic changes during experimental evolution.

3.5 | Mutations in structural genes were predominant in evolved T4 populations

Mutations during evolution tended to cluster in regions of the T4 genome containing genes that code for structural proteins. Furthermore, of the 62 polymorphisms that reached a frequency of 50% or greater, all but four occurred in structural genes. To formally test whether different regions of the genome experienced different rates of mutation, and if the rates also depended on the evolutionary history of the population, a Scheirer–Ray–Hare (SRH) nonparametric two-way ANOVA (Sokal & Rohlf, 2011) was performed. First, the number of nucleotide sites that each functional category occupies in the genome was determined. From this, the mutation rate (number of mutations per nucleotide site) of each category was calculated for the 15 evolved populations. Evolutionary history, functional category, and their interaction were specified as factors in the SRH nonparametric two-way ANOVA. This analysis showed that the rate of mutation was different across functional gene categories ($p < .001$). There was neither a significant effect for evolutionary history ($p = .588$) nor for interactions between functional category and history ($p = .789$).

To examine pairwise comparisons between functional categories with regards to mutation rate, we used a Dunn's test, which revealed that only comparisons involving the structural gene category were significant ($p < .01$). Specifically, this indicated that the mutation rate of the structural gene category was significantly higher (i.e., mutations were overrepresented in structural genes) than all other categories.

4 | DISCUSSION

In this study, we performed experimental evolution using *Escherichia virus T4* to examine the phenotypic and molecular manifestations of niche breadth evolution. Our findings demonstrate that niche breadth evolution led to measurable changes in phage productivity. For populations grown on *E. coli* C, productivity on *E. coli* C increased while productivity decreased on both *E. coli* B and K-12, indicating that adaptation on *E. coli* C led to reduced performance on both the original and unselected hosts. These results conform to expectations, set by other seminal studies, where evolved populations improve performance in the selective environment at the expense of diminished performance in alternate environments (Turner & Elena, 2000). For the alternating host evolved populations, the magnitude of increased productivity on *E. coli* C was smaller than that of the populations that only experienced the same host, which suggests that exposure to two hosts and temporal variability limited adaptation on *E. coli* C. This result also conforms to theoretical expectations; specialists are predicted to evolve faster than generalists because the time to fixation of favorable alleles is shorter for specialists (Whitlock, 1996).

4.1 | Some experimental populations deviated from the expectations of simple trade-off models

In contrary to the results of the *E. coli C*-exposed populations, the observed changes in productivity (on *E. coli* K-12) for the *E. coli* K-12 and alternating host populations offered surprising results. For example, these treatment populations demonstrated decreased productivity on *E. coli* K-12, despite being experimentally exposed to this host. These results were not only unforeseen, but also deviate from theoretical expectations. We predicted that evolution on *E. coli* K-12 would lead to higher productivity with the single host exposed populations performing better than the alternating host populations. Instead, we observed decreased *E. coli* K-12 productivity with no significant differences between the single (*E. coli* K-12) and alternating host (*E. coli* K-12/*E. coli* B) histories. Though empirical evidence from previous viral experimental evolution studies have contradicted theory and found no cost associated with generalism (Bedhomme et al., 2012; Novella et

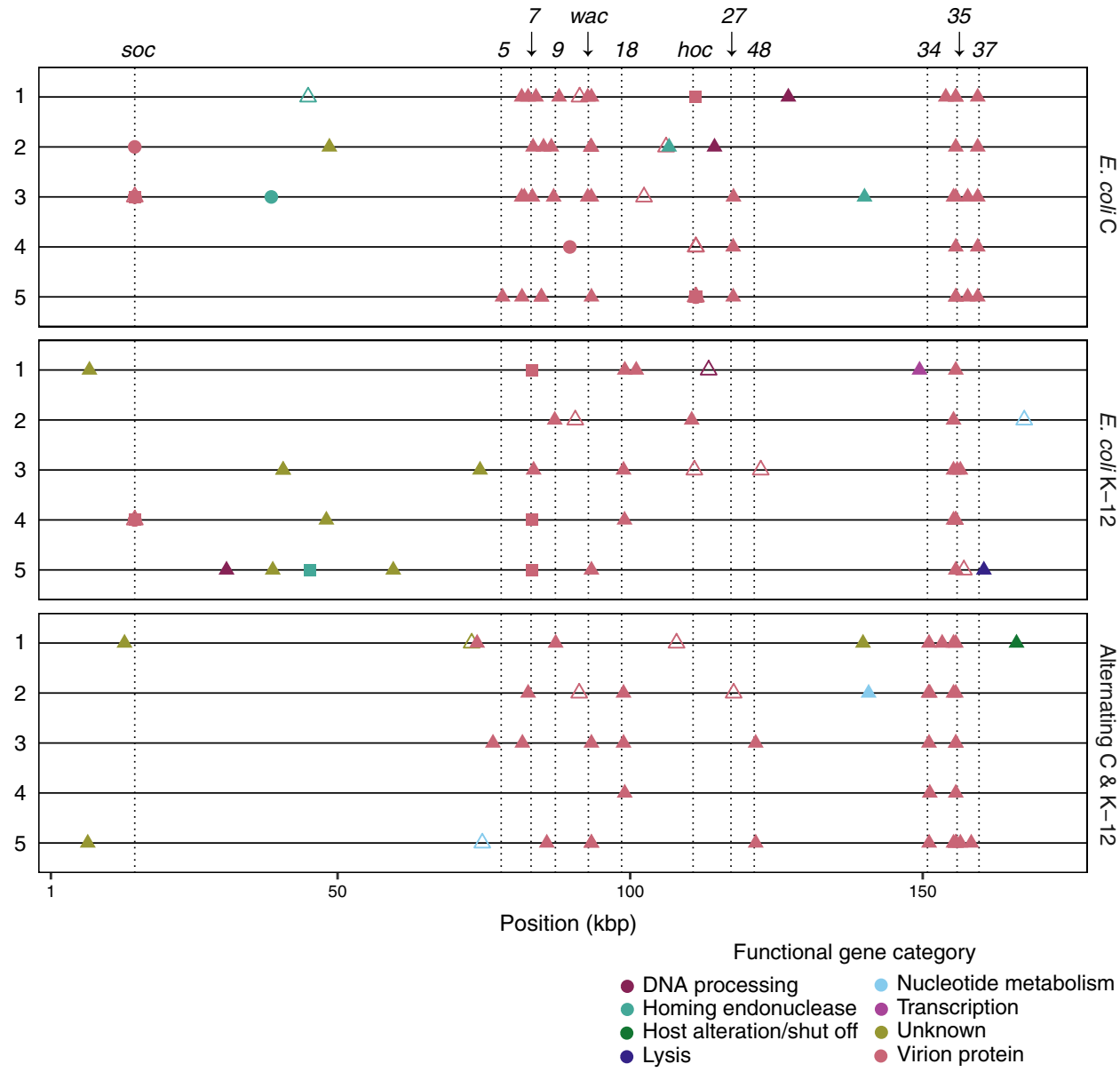

FIGURE 4 *The distribution of new mutations detected in the evolved phage populations.* Panels indicate one of three evolutionary histories, and lines within panels represent particular populations within an evolutionary history; numbers for each horizontal line correspond to the numbered populations that underwent passaging. Each point represents a new mutation (relative to the ancestor) detected at ≥5% frequency. Point shape indicates type of mutation (filled triangles: nonsynonymous; empty triangles: synonymous; circles: indel; squares: xNPs (multiple adjacent nucleotide polymorphisms); and diamonds: intergenic). Colors indicate functional gene category; labels above the top panel and dashed lines denote relative positions of virion structural genes

al., 1999; Turner & Elena, 2000), our results offer a unique departure from past findings. This raises an important question specific to our system: why would T4 passaged on *E. coli* K-12 evolve lower productivity on its selective host? One simple explanation is that productivity did not improve because it was not the target of selection, which undermines the neat (and convenient) equivalence between productivity and reproductive fitness. In contexts where competition is more synonymous with fitness, one might expect productivity to be completely decoupled from evolution. Indeed, prior studies have suggested that productivity can be negatively correlated with competitive ability in T4 in the setting of experimental evolution (Kerr et al., 2006).

4.2 | Study limitations

As with any exercise in experimental evolution used to investigate an ecological phenomenon, there are many limitations that can affect our interpretations and conclusions. The chief concern is that measurements made in the laboratory may not be relevant to organisms in their natural context. However contrived, evolutionary and ecological phenomena still apply to our experimental microcosm, which makes it nevertheless useful for examining ecological questions. Consequently, we are comfortable interpreting our results and discussing them in light of broader ecological theory. Next, our study did not measure

changes in phage fitness, but rather, phage productivity. Though this trait can be closely associated with phage fitness and has been previously used as a proxy for fitness (Morley et al., 2015; Turner, Draghi, & Wilpiszeski, 2012), it is clear from our findings that assuming this equivalence is not always appropriate in our system. Importantly, this suggests that the productivity to fitness equivalence might not exist for other virus–host systems. Lastly, our interpretations should consider the potentially complicating role of phenotypic plasticity in these results, as phage phenotypes may be moderated by the host encountered. For example, previous work in T4 has shown that expression of T4 mutant phenotypes can be moderated by bacterial host strain (Benzer, 1957).

4.3 | Evolutionary genomics data reveals evidence for selection

We observed genetic signatures that are suggestive of selection shaping the evolved populations during niche breadth evolution. Specifically, the high dN/dS ratio, along with the observation that few nonsynonymous mutations reached fixation, indicates selection. The genotypic evidence is suggestive of positive selection as the source of elevated rate of nonsynonymous mutations in structural genes (for a more detailed discussion of other plausible causes, such as mutation bias, see the Appendix A). Though mutation bias can influence the nature of mutations that arrive, newly introduced mutations are still subject to elimination or fixation through the processes of drift and selection. As such, it is probable that fixed (or high frequency) nonsynonymous mutations are of adaptive significance (even if their presence was influenced by mutation bias).

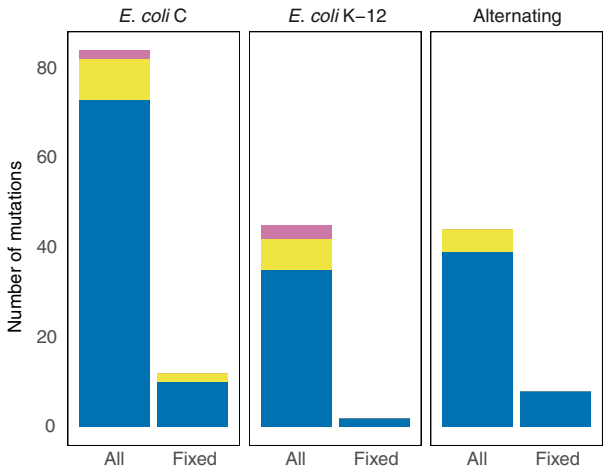

FIGURE 5 *Classification of mutations*. Panels indicate one of three histories; categories within panels indicate the total number of observed (>5%) and fixed (>80%) mutations for the five parallel populations within each history. Bar colors represent the type of mutation for each category: intergenic, synonymous, and nonsynonymous

4.4 | The role of structural genes in bacteriophage niche breadth evolution

Our findings demonstrate that structural genes play a central role in niche breadth evolution: i) The overwhelming majority (82%) of new mutations occurred in structural genes; ii) nearly all (94%) high frequency mutations (>50%) occurred in structural genes; and iii) we detected a significantly higher mutation rate in structural genes. Notably, these rates did not differ across evolutionary histories, which indicates that structural genes are important niche breadth evolution, regardless of the host(s) encountered and level of temporal variability of the environment. Structural genes encode for four different types of virion proteins: capsid, neck, tail, and tail fibers (Miller et al., 2003). Of the 142 new mutations detected in structural genes, 44% occurred in genes coding for tail fiber proteins. We observed mutations in gene *37*, which encodes the distal subunit of the LTF (gp37) that directly interacts with bacterial receptors (Bartual et al., 2010). This supports previous evidence suggesting that mutation in gene *37* can alter the niche breadth of T4 (Tétart, Repoila, Monod, & Krisch, 1996). Interestingly, the majority of mutations (74%) detected in LTF genes occurred in the genes encoding the LTF proximal subunits (i.e., gp34 and gp35). This suggests that structures that are only indirectly responsible for host recognition are also important to niche breadth evolution. Mutations in tail genes accounted for 30% of structural mutations; the great majority of those mutations (82%) occurred in genes that code for various baseplate components (e.g., genes *5–10*, *27*, *48*, and *54*). Mutations in baseplate genes occurred across all three evolutionary histories, in nearly every population (14 out of 15). This suggests that the baseplate, which regulates infection (Yap

TABLE 3 The total number of observed and fixed[a] mutations in the 15 sequenced populations, grouped by evolutionary history and sorted by type. The percentage of mutations observed and fixed in a given type are shown in parentheses

History	Category	All	Nonsyn	Syn	Intergenic
Escherichia coli C	All	85	74 (87%)	9 (11%)	2 (2%)
	Fixed	12	10 (83%)	2 (17%)	0
Escherichia coli K–12	All	45	35 (78%)	7 (15%)	3 (7%)
	Fixed	1	1 (100%)	0	0
Alternating	All	44	39 (89%)	5 (11%)	0
	Fixed	8	8 (100%)	0	0

[a]Mutations are classified as fixed if they reach a frequency >80%.

et al., 2016), may serve an important role in the evolution of niche breadth. The remaining structural mutations were detected in six genes that code for capsid proteins, with the vast majority (90%) occurring in two of those six genes: *soc* (small outer capsid) and *hoc* (head outer capsid). This suggests that soc and hoc proteins, which provide stability to the capsid (Fokine et al., 2004), may also be important to niche breadth evolution. For those interested in a more detailed discussion of mutations, for example, parallel substitutions or distribution across populations, please refer to Appendix A.

5 | CONCLUSIONS

In this study, we used experimental evolution of *Escherichia virus T4* to characterize the phenotypic and molecular changes associated with niche breadth evolution. Our findings indicate that populations evolved measurable and meaningful changes in phage productivity. These phenotypic results confirmed some and contradicted other theoretical expectations, which demonstrates the complexity of niche breadth evolution, and the dubiousness of theoretical expectations: Whether generalism truly comes at the expense of high productivity in individual niches is likely context and system-specific.

Genomic sequencing of evolved populations enabled us to detect a significantly higher rate of mutation in structural genes. Notably, mutation rates of structural genes were similar across evolutionary histories, which indicates that selection in structural genes is important to niche breadth evolution, regardless of conditions that promoted a particular ecological strategy (specialism or generalism). Our study presents compelling evidence that structural genes serve an important role in how phage evolve different niche breadth strategies. This finding further supports the importance of phage structure in the evolution of niche breadth, a result that may have implications for public health surveillance and in therapy. For example, insofar as variation in structural genes is associated with different niche breadth exploitation, perhaps these genes can be manipulated to facilitate a phage's ability to fight particular infections, as in phage therapy (Kortright, Chan, Koff, & Turner, 2019). In addition, if phage genes are associated with expansion of host range, then they may be candidates for a "watch list" approach in disease surveillance, where natural populations are surveyed for mutations associated with exploiting new hosts (Patel, Quates, Johnson, & Ytreberg, 2019).

ACKNOWLEDGMENTS

JYP was supported by the National Science Foundation Graduate Research Fellowship Program under Grant No. DGE1745303. The authors would like to thank K. Namgyal for help with media preparation and serial propagation, R. Hopkins, E. Wolkovich, and S. Worthington for consultation on statistical approaches. The authors would like to thank T. Sackton for advice on sequencing and linear models, Claire Reardon for advice on library preparation and sequencing, and M. Desai for providing laboratory space and reagents for library preparation. CBO acknowledges funding support from NSF RII Track-2 FEC award number 1736253.

CONFLICT OF INTERESTS

None declared.

AUTHOR CONTRIBUTIONS

Conceptualization: Jenny Y. Pham, C. Brandon Ogbunugafor, and Daniel L. Hartl. Formal analysis: Jenny Y. Pham and Alex N. Nguyen Ba. Funding acquisition: Jenny Y. Pham, C. Brandon Ogbunugafor, and Daniel L. Hartl. Writing—original draft preparation: Jenny Y. Pham, C. Brandon Ogbunugafor, and Daniel L. Hartl. Writing—review and editing: Jenny Y. Pham, Alex N. Nguyen Ba, C. Brandon Ogbunugafor, and Daniel L. Hartl.

ETHICS STATEMENT

None required.

ORCID

C. Brandon Ogbunugafor https://orcid.org/0000-0002-1581-8345
Daniel L. Hartl https://orcid.org/0000-0002-0302-306X

DATA AVAILABILITY STATEMENT

Phenotypic data can be found on Figshare:

Data from Figure 2a: https://doi.org/10.6084/m9.figshare.10025312.v1

Data from Figure 2b: https://doi.org/10.6084/m9.figshare.10025321.v3

Data from Figure 3: https://doi.org/10.6084/m9.figshare.10025327.v1

DNA sequence data for T4 populations presented in this study can be found on the Sequence Read Archive (https://www.ncbi.nlm.nih.gov/sra/), Accession PRJNA578899.

REFERENCES

References which are present in both "Main reference list/text citations" and "Appendix References/appendix text citations" are indicated by*.

*Abedon, S. T., Herschler, T. D., & Stopar, D. (2001). Bacteriophage latent-period evolution as a response to resource availability. *Applied and Environmental Microbiology*, *67*(9), 4233–4241. https://doi.org/10.1128/aem.67.9.4233-4241.2001

*Bartual, S. G., Otero, J. M., Garcia-Doval, C., Llamas-Saiz, A. L., Kahn, R., Fox, G. C., & van Raaij, M. J. (2010). Structure of the bacteriophage T4 long tail fiber receptor-binding tip. *Proceedings of the National Academy of Sciences of the United States of America*, *107*(47), 20287–20292. https://doi.org/10.1073/pnas.1011218107

*Bedhomme, S., Lafforgue, G., & Elena, S. F. (2012). Multihost experimental evolution of a plant RNA virus reveals local adaptation and host-specific mutations. *Molecular Biology and Evolution*, *29*(5), 1481–1492. https://doi.org/10.1093/molbev/msr314

*Fokine, A., Chipman, P. R., Leiman, P. G., Mesyanzhinov, V. V., Rao, V. B., & Rossmann, M. G. (2004). Molecular architecture of the prolate head of bacteriophage T4. *Proceedings of the National Academy of*

Sciences of the United States of America, *101*(16), 6003–6008. https://doi.org/10.1073/pnas.0400444101

*Tétart, F., Repoila, F., Monod, C., & Krisch, H. (1996). Bacteriophage T4 host range is expanded by duplications of a small domain of the tail fiber adhesin. *Journal of Molecular Biology*, *258*, 726–731. https://doi.org/10.1006/jmbi.1996.0281

*Yap, M. L., Klose, T., Arisaka, F., Speir, J. A., Veesler, D., Fokine, A., & Rossmann, M. G. (2016). Role of bacteriophage T4 baseplate in regulating assembly and infection. *Proceedings of the National Academy of Sciences of the United States of America*, *113*(10), 2654–2659. https://doi.org/10.1073/pnas.1601654113

*Yu, F., & Mizushima, S. (1982). Roles of lipopolysaccharide and outer membrane protein OmpC of Escherichia coli K-12 in the receptor function for bacteriophage T4. *Journal of Bacteriology*, *151*(2), 718–722.

Bates, D., Mächler, M., Bolker, B., & Walker, S. (2015). Fitting linear mixed-effects models using lme4. *Journal of Statistical Software*, *67*(1), 1–48. https://doi.org/10.18637/jss.v067.i01

Baym, M., Kryazhimskiy, S., Lieberman, T. D., Chung, H., Desai, M. M., & Kishony, R. (2015). Inexpensive multiplexed library preparation for megabase-sized genomes. *PLoS ONE*, *10*(5), 1–15. https://doi.org/10.1371/journal.pone.0128036

Benzer, S. (1957). The elementary units of heredity. *The elementary units of heredity*.

Bolger, A. M., Lohse, M., & Usadel, B. (2014). Trimmomatic: A flexible trimmer for Illumina sequence data. *Bioinformatics*, *30*(15), 2114–2120. https://doi.org/10.1093/bioinformatics/btu170

Carrasco, P., de la Iglesia, F., & Elena, S. F. (2007). Distribution of fitness and virulence effects caused by single-nucleotide substitutions in Tobacco Etch virus. *Journal of Virology*, *81*(23), 12979–12984. https://doi.org/10.1128/JVI.00524-07

Coleman, J. R., Papamichail, D., Skiena, S., Futcher, B., Wimmer, E., & Mueller, S. (2008). Virus attenuation by genome-scale changes in codon pair bias. *Science*, *320*(5884), 1784–1787.

Cooper, L. A., & Scott, T. W. (2001). Differential evolution of eastern equine encephalitis virus populations in response to host cell type. *Genetics*, *157*(4), 1403–1412.

Crill, W. D., Wichman, H. A., & Bull, J. (2000). Evolutionary reversals during viral adaptation to alternating hosts. *Genetics*, *154*(1), 27–37.

Cuevas, J. M., Domingo-Calap, P., & Sanjuan, R. (2012). The fitness effects of synonymous mutations in DNA and RNA viruses. *Molecular Biology and Evolution*, *29*(1), 17–20. https://doi.org/10.1093/molbev/msr179

Deatherage, D. E., & Barrick, J. E. (2014). Identification of mutations in laboratory-evolved microbes from next-generation sequencing data using breseq. *Methods in Molecular Biology*, *1151*, 165–188. https://doi.org/10.1007/978-1-4939-0554-6_12

Demerec, M., & Fano, U. (1944). Bacteriophage-resistant mutants in Escherichia coli. *Genetics*, *19*, 119–136.

Duffy, S., Burch, C. L., & Turner, P. E. (2007). Evolution of host specificity drives reproductive isolation among RNA viruses. *Evolution*, *61*(11), 2614–2622. https://doi.org/10.1111/j.1558-5646.2007.00226.x

Enav, H., Kirzner, S., Lindell, D., Mandel-Gutfreund, Y., & Béjà, O. (2018). Adaptation to sub-optimal hosts is a driver of viral diversification in the ocean. *Nature Communications*, *9*(1), 4698. https://doi.org/10.1038/s41467-018-07164-3

Fokine, A., Zhang, Z., Kanamaru, S., Bowman, V. D., Aksyuk, A. A., Arisaka, F., … Rossmann, M. G. (2013). The molecular architecture of the bacteriophage T4 neck. *Journal of Molecular Biology*, *425*(10), 1731–1744. https://doi.org/10.1016/j.jmb.2013.02.012

Fox, J., & Weisberg, S. (2011). *An R companion to applied regression*, 2nd ed. Thousand Oaks, CA: Sage.

Hadas, H., Einav, M., Fishov, I., & Zaritsky, A. (1997). Bacteriophage T4 development depends on the physiology of its host Escherichia coli. *Microbiology*, *143*, 179–185.

Ishii, T., & Yanagida, M. (1977). The two dispensable structural proteins (soc and hoc) of the T4 phage capsid; their purification and properties, isolation and characterization of the defective mutants, and their binding with the defective heads in vitro. *Journal of Molecular Biology*, *109*(4), 487–514.

Kassen, R. (2002). The experimental evolution of specialists, generalists, and the maintenance of diversity. *Journal of Evolutionary Biology*, *15*(2), 173–190. https://doi.org/10.1046/j.1420-9101.2002.00377.x

Kerr, B., Neuhauser, C., Bohannan, B. J., & Dean, A. M. (2006). Local migration promotes competitive restraint in a host-pathogen 'tragedy of the commons'. *Nature*, *442*(7098), 75–78. https://doi.org/10.1038/nature04864

Kortright, K. E., Chan, B. K., Koff, J. L., & Turner, P. E. (2019). Phage therapy: A renewed approach to combat antibiotic-resistant bacteria. *Cell Host & Microbe*, *25*(2), 219–232. https://doi.org/10.1016/j.chom.2019.01.014

Kostyuchenko, V. A., Leiman, P. G., Chipman, P. R., Kanamaru, S., van Raaij, M. J., Arisaka, F., … Rossmann, M. G. (2003). Three-dimensional structure of bacteriophage T4 baseplate. *Natural Structural Biology*, *10*(9), 688–693. https://doi.org/10.1038/nsb970

Kostyuchenko, V. A., Navruzbekov, G. A., Kurochkina, L. P., Strelkov, S. V., Mesyanzhinov, V. V., & Rossmann, M. G. (1999). The structure of bacteriophage T4 gene product 9: the trigger for tail contraction. *Structure*, *7*(10), 1213–1222.

Kutnjak, D., Elena, S. F., & Ravnikar, M. (2017). Time-sampled population sequencing reveals the interplay of selection and genetic drift in experimental evolution of potato virus Y. *Journal of Virology*, *91*(16), e00690-17. https://doi.org/10.1128/JVI.00690-17

Leiman, P. G., Arisaka, F., van Raaij, M. J., Kostyuchenko, V. A., Aksyuk, A. A., Kanamaru, S., & Rossmann, M. G. (2010). Morphogenesis of the T4 tail and tail fibers. *Virology Journal*, *7*(355), 1–28.

Lenski, R. E., Rose, M. R., Simpson, S. C., & Tadler, S. C. (1991). Long-Term Experimental Evolution in Escherichia coli. I. Adaptation and Divergence Durng 2,000 Generations. *American Society of Naturalists.*, *138*(6), 1315–1341.

Lenth, R. V. (2016). Least-squares means: The R package lsmeans. *Journal of Statistical Software*, *69*(1), 1–33. https://doi.org/10.18637/jss.v069.i01

Letarov, A., Manival, X., Desplats, C., & Krisch, H. M. (2005). gpwac of the T4-type bacteriophages: structure, function, and evolution of a segmented coiled-coil protein that controls viral infectivity. *Journal of Bacteriology*, *187*(3), 1055–1066. https://doi.org/10.1128/JB.187.3.1055-1066.2005.

Mangiafico, S. (2018). *rcompanion: Functions to Support Extension Education Program Evaluation*. R package version 1.11.3.

McDonald, M. J., Rice, D. P., & Desai, M. M. (2016). Sex speeds adaptation by altering the dynamics of molecular evolution. *Nature*, *531*(7593), 233–236. https://doi.org/10.1038/nature17143

Miller, E. S., Kutter, E., Mosig, G., Arisaka, F., Kunisawa, T., & Ruger, W. (2003). Bacteriophage T4 Genome. *Microbiology and Molecular Biology Reviews*, *67*(1), 86–156. https://doi.org/10.1128/mmbr.67.1.86-156.2003

Miralles, R., Moya, A., & Elena, S. F. (2000). Diminishing Returns of Population Size in the Rate of RNA Virus Adaptation. *Journal of Virology*, *74*(8), 3566–3571.

Monod, J. (1949). The growth of bacterial cultures. *Annual Reviews in Microbiology*, *3*(1), 371–394.

Morley, V. J., Mendiola, S. Y., & Turner, P. E. (2015). Rate of novel host invasion affects adaptability of evolving RNA virus lineages. *Proceedings of the Royal Society B*, *282*(1813), 20150801. https://doi.org/10.1098/rspb.2015.0801

Novella, I. S., Clarke, D. K., Quer, J., Duarte, E. A., Lee, C. H., Weaver, S. C., … Holland, J. J. (1995). Extreme fitness differences in mammalian and insect hosts after continuous replication of vesicular stomatitis virus in sandfly cells. *Journal of Virology*, *69*(11), 6805–6809.

Novella, I. S., Hershey, C. L., Escarmis, C., Domingo, E., & Holland, J. J. (1999). Lack of evolutionary stasis during alternating replication of an arbovirus in insect and mammalian cells. *Journal of Molecular Biology*, *287*(3), 459–465. https://doi.org/10.1006/jmbi.1999.2635

Ogle, D. H. (2018). *FSA: Fisheries Stock Analysis*. R package version 0.8.19.

Patel, J. S., Quates, C. J., Johnson, E. L., & Ytreberg, F. M. (2019). Expanding the watch list for potential Ebola virus antibody escape mutations. *PLoS ONE*, *14*(3), e0211093. https://doi.org/10.1371/journal.pone.0211093

R Development Core Team (2017). *R: A language and environment for statistical computing*. Vienna, Austria: R Foundation for Statistical Computing.

Ren, Z.-J., & Black, L. W. (1998). Phage T4 SOC and HOC display of biologically active, full-length proteins on the viral capsid. *Gene*, *215*(2), 439–444.

Sokal, R. R., & Rohlf, F. J. (2011). *Biometry: The principles and practice of statistics in biological research*, 4th ed. New York, NY: W. H. Freeman and Co.

Stoltzfus, A., & McCandlish, D. M. (2017). Mutational Biases Influence Parallel Adaptation. *Molecular Biology and Evolution*, *34*(9), 2163–2172. https://doi.org/10.1093/molbev/msx180

Terzaghi, B. E., Terzaghi, E., & Coombs, D. (1979). The role of the collar/whisker complex in bacteriophage T4D tail fiber attachment. *Journal of Molecular Biology*, *127*(1), 1–14.

Turner, P. E., Draghi, J. A., & Wilpiszeski, R. (2012). High-throughput analysis of growth differences among phage strains. *Journal of Microbiol Methods*, *88*(1), 117–121. https://doi.org/10.1016/j.mimet.2011.10.020

Turner, P. E., & Elena, S. F. (2000). Cost of host radiation in an RNA virus. *Genetics*, *156*, 1465–1470.

Whitlock, M. C. (1996). The red queen beats the jack-of-all-trades: The limitations on the evolution of phenotypic plasticity and niche breadth. *The American Naturalist*, *148*, S65–S77. https://doi.org/10.1086/285902

Wichman, H. A., Millstein, J., & Bull, J. J. (2005). Adaptive molecular evolution for 13,000 phage generations: A possible arms race. *Genetics*, *170*(1), 19–31. https://doi.org/10.1534/genetics.104.034488

Wood, W. B., Eiserling, F. A., & Crowther, R. A.. (1994). Long tail fibers: genes, proteins, structure and assembly. In J. D. Karam (Ed.), *Molecular biology of bacteriophage T4* (pp. 282–290). Washington, DC: American Society for Microbiology.

Zuur, A. F., Ieno, E. N., & Elphick, C. S. (2010). A protocol for data exploration to avoid common statistical problems. *Methods in Ecology and Evolution*, *1*(1), 3–14. https://doi.org/10.1111/j.2041-210X.2009.00001.x****

How to cite this article: Pham JY, Ogbunugafor CB, Nguyen Ba AN, Hartl DL. Experimental evolution for niche breadth in bacteriophage T4 highlights the importance of structural genes. *MicrobiologyOpen*. 2020;9:e968. https://doi.org/10.1002/mbo3.968

APPENDIX A

In this section, we offer extended discussion points and analyses related to the findings presented in the main text. In particular, this section provides additional detail on several of the molecular findings presented in the main text.

QUANTIFYING THE NUMBER OF GENERATIONS

Due to exponential growth via binary fission, the number of bacterial generations (*G*) is calculated by the equation below, with B_0 representing the initial number of bacteria and B_F representing the number of bacteria at the end of a time interval (Lenski, Rose, Simpson, & Tadler, 1991; Monod, 1949):

$$B_F = B_0 \times 2^G \quad (1)$$

Bacteriophage also grow exponentially, with the number of generations being determined by burst size (the number of phage progeny produced per infected bacterium) rather than binary fission. The bacterial equation can then be modified to suit phage, with V_0 representing the initial number of phage, V_F representing the number of phage at the end of a time interval, and *R* representing burst size (Abedon et al., 2001; Miralles, Moya, & Elena, 2000):

$$V_F = V_0 \times R^G \quad (2)$$

The burst size for T4 on *E. coli* B has been previously determined to be approximately 110 PFU/ml (Hadas, Einav, Fishov, & Zaritsky, 1997), and a typical overnight infection of T4 in *E. coli* B results in 100,000 × growth (based on experimental data from Figure 2a), hence the number of generations is ~2.5. Though this calculation can provide a general impression of the number of T4 generations which occurred during experimental evolution, it is an imperfect estimate. A more accurate estimate would require knowledge of the burst size on the selected host (which may be different than the burst size on *E. coli* B) and the number of phages added and produced during serial passaging infections (which may change from one passage to another).

NOTES ON ANALYSIS OF MUTATIONS LOCATED IN CAPSID GENES

The majority of mutations in outer capsid genes were detected in the *hoc* gene. In particular, one *E. coli* C evolved lineage sustained 24 *hoc* mutations that occurred at nearly equivalent frequencies (53%–57%) and were observed in nucleotide positions which were in close proximity or adjacent to each other. Visualization of sequencing reads containing the relevant positions revealed that these polymorphisms appeared as a block (reads contained all or none of the mutations), which indicates a major but singular mutational event. A second set of polymorphisms detected at approximately 77% frequency was observed in a different *E. coli* C evolved lineage. This six base pair mutation resulted in two amino acid substitutions; again, visualization of reads revealed that these mutations appeared as a block. These observations are particularly interesting in light of functional characterizations of *soc* and *hoc*. Viable T4 mutants missing either or both proteins have been isolated, demonstrating that these proteins are nonessential for phage growth (Ishii & Yanagida, 1977). In fact, the dispensable nature of these proteins provided the basis for T4-phage display, a technique in which novel protein and polypeptide sequences are inserted into *soc* and/or *hoc*, resulting in display on the phage surface for identification and characterization (Ren & Black, 1998). However, soc proteins are known to provide stability to the capsid in extreme pH and temperatures, whereas hoc proteins have a

more marginal effect on stability (Fokine et al., 2004). This indicates that the mutations we observed are unlikely to be severely deleterious, but it is presently unclear if they are selectively neutral or beneficial. However, the two *E. coli* C evolved lineages which sustained these mutations were also the lineages that experienced the greatest magnitude of productivity increase on *E. coli* C (see lineages 1 and 5 of Figure 4). Furthermore, lineage 5 of the *E. coli* C history sustained two additional fixed nonsynonymous mutations in the *hoc* gene. These observations are possibly a coincidence. Conversely, they could indicate a potential beneficial effect (e.g., increased virion stability or rate of capsid morphogenesis).

The adsorption of T4 on *E. coli* is initiated by the tail fibers, beginning with a reversible interaction between the long tail fibers (LTF) and receptors on the bacterial cell surface (lipopolysaccharide and/or OmpC proteins), followed by irreversible binding of the short tail fibers (STF) (Yu & Mizushima, 1982; Kostyuchenko et al., 1999). The T4 tail fiber proteins are thus responsible for interactions that are the gatekeepers of infection; following adhesion, phage DNA is injected into the bacterium for replication and subsequent completion of the lytic life cycle. The LTF is a multiprotein complex composed of four different gene products: gp34, gp35, gp36, and gp37. Gp36 and gp37 are the subunits that form the distal half of the LTF, with gp37 acting as the portion of the LTF that is directly involved with bacterial receptor recognition. Gp34 and gp35 are the subunits that form the proximal half of the LTF, with gp35 forming the "kneecap" hinge and gp34 interacting with the phage baseplate (Bartual et al., 2010; Leiman et al., 2010).

Previous work has shown that duplications in gene *37* (encodes gp37) expands the T4 host range to include *Yersinia*, a bacterial genus that wild-type laboratory strains of T4 cannot infect (Tétart et al., 1996). We observed mutations in genes *12* (encodes STF) and *37*; however, all three mutations observed in *12* were synonymous, and only present in three lineages at frequencies <13%, while eight of the nine mutations observed in *37* were nonsynonymous and occurred in seven lineages at frequencies between 5% and 100%, across all three histories. Notably, one codon position in *37* was substituted with two different amino acid residues: Y953H and Y953F; these substitutions only occurred in the *E. coli* C history, with the first detected in three lineages, and the latter detected in two lineages (Appendix B). The Y953H mutation was fixed across the three lineages in which it was detected while the Y953F mutation occurred at frequencies of 17% and 25%. It is possible that these mutations may be specifically adaptive to *E. coli* C because replacements at this particular position only occurred in one evolutionary history.

One particular nonsynonymous mutation (G323D) in gene *35* was detected in 12 of the 15 lineages. Two of the three lineages without this mutation sustained a different nonsynonymous substitution (T193M) in gene *35*, and three lineages displayed both substitutions. The G323D substitution was fixed in four lineages (two in the alternating history and one in each single host history) and detected at high frequency (≥60%) in five other lineages (across three histories). The high frequencies and degree of parallelism of the G323D substitution are striking and suggests an interplay between mutation bias and selection. Given the interaction between LTF proteins, one might hypothesize that mutations in gene *35* are compensatory to mutations in gene *37*, but the presence of eight lineages with polymorphisms detected in gene *35* and not gene *37* challenges that hypothesis. Rather, given the distribution and high frequency of G323D observed across all three histories, we hypothesize that this substitution is universally beneficial to phage growth capabilities.

In the case of gene *34*, a different pattern emerged: There were no parallel mutations; however, nearly all of the mutations in this gene (8 out of 9) were sustained by lineages evolved in the alternating host environment. Different substitutions at the same codon position were detected in four different lineages. In two of those lineages, the substitutions A89T and A89V were, respectively, observed at frequencies of 7% and 51%. Separately, the substitutions G133S and G133R were observed in two other lineages; the first amino acid replacement reached a frequency of 76%, while the latter became fixed in the population. These observations indicate the possibility that mutations of gene *34* are of adaptive significance to a temporally variable host environment (i.e., generalist strategy).

Another nonsynonymous mutation (R417H) that displayed high frequencies with parallelism (6 out of 15 lineages, across three histories) occurred in the *wac* gene. The R417H substitution reached fixation in one lineage and high frequency (≥60%) in a second lineage (frequencies in other lineages were between 6% and 41%). Furthermore, we observed other fixed substitutions in *wac*: V207E in one *E. coli* C evolved lineage, and V414D in one alternating host evolved lineage. The gene product gpwac forms six whisker fibers that radiate from the phage neck, in manner akin to a "collar." Gpwac is multifunctional; during morphogenesis, the whiskers facilitate the binding of LTF to the phage baseplate. In extracellular conditions, gpwac performs an important regulatory function: The whiskers bind the LTF, holding them in a retracted position, thus acting as a rudimentary environmental sensor that prevents adsorption in conditions unfavorable for infection (*e.g.*, low pH) (Fokine et al., 2013; Letarov, Manival, Desplats, & Krisch, 2005; Terzaghi, Terzaghi, & Coombs, 1979; Wood, Eiserling, & Crowther, 1994). Mutations in *wac* may be beneficial; however, it is unclear how the traits that are governed by gpwac were affected. It is conceivable that mutations in the LTF (along with mutations in the baseplate, which were also observed) required accommodation during morphogenesis, though it is also possible that the capacity of environmental sensing was affected.

Of the mutations that occurred in tail genes, 82% occurred in genes that code for various baseplate components (*5–10*, *27*, *48*, and *54*). In total, three nonsynonymous mutations and one 12 bp indel in baseplate genes reached fixation (all occurred separately in different lineages). Additionally, mutations in baseplate genes occurred across all three evolutionary histories in nearly every lineage (14 out of 15). The phage baseplate is a complex multiprotein structure that is attached to the contractile tail. The LTF and STF

are attached to the baseplate, which changes conformation along with the irreversible binding of STF (Kostyuchenko et al., 2003). This event triggers tail sheath contraction, which drives the tail tube into the bacterial inner membrane, where phage genomic DNA is injected into the host cytoplasm. Thus, the baseplate can be regarded as the nerve center of T4, transmitting signals from the tail fibers to the phage capsid for release of DNA (Yap et al., 2016). Given the importance of the baseplate in the coordination of events that lead to infection, it is possible that mutations in baseplate genes were either compensatory to mutations in the LTF or provided an unrelated selective benefit.

We emphasize that the relationships discussed here between detected polymorphisms and changes in host use and phage growth are plausible but nevertheless speculative. The observations do provide reasonable hypotheses and justifications to further explore the effects of these mutations through site-directed mutagenesis experiments to determine whether these mutational effects are of adaptive significance to a particular host or provide universal benefit in phage growth capabilities. Although the discussion focused on particular mutations of interest, it is possible that the effects of these mutations were modulated by epistatic interactions with other polymorphisms.

ON THE POSSIBILITY FOR MUTATION BIAS IN EVOLVED POPULATIONS

The overrepresentation of new synonymous polymorphisms in structural genes can imply the presence of mutation bias and/or selection for synonymous mutations. Previous work has demonstrated that synonymous substitutions can have non-neutral effects in RNA viruses (Bedhomme et al., 2012; Carrasco, de la Iglesia, & Elena, 2007; Coleman et al., 2008). However, site-directed mutagenesis indicates that selection at synonymous sites is very weak in DNA viruses (Cuevas, Domingo-Calap, & Sanjuan, 2012). In our study, the observed transition:transversion ratio significantly exceeded the null expectation; when this observation is considered with the aforementioned evidence, it seems unlikely that selection for synonymous mutations occurred. Below, we describe how mutation bias was measured and evaluate the evidence for it in the study populations.

ANALYSIS OF MUTATION BIAS

All polymorphisms ≥5% that resulted in base pair substitutions were considered in this analysis. The transition:transversion ratio of paths was calculated by tabulating the number of substitutions that occurred. The transition:transversion ratio of events was calculated by tabulating the number of instances for each substitution. For example, the substitution CGC → CAC represents one path but six events because it was observed in six populations. Depending on model details, the expected ratio of transition:transversion mutations can range between 0.4 and 0.5 (Stoltzfus & McCandlish, 2017). In the simplest scenario, the null expectation is 0.5 because every nucleotide is subject to one transition and two transversions. We chose the estimate of 0.5 because it is the most conservative. For the purposes of statistical testing, the transition:transversion ratio was calculated separately for each evolved population. A Pearson's chi-square test was performed to determine if the observed transition:transversion ratios differed from the null expectation. This analysis was performed in Microsoft Excel version 15.20. It is important to note that in the absence of mutation accumulation experiments, we cannot fully conclude that there is true mutation bias.

EVIDENCE FOR MUTATION BIAS

We further explored the processes responsible for the overrepresentation of mutations in structural genes by repeating the SRH nonparametric two-way ANOVA separately on synonymous and nonsynonymous mutations. In this analysis, we tested whether different regions of the genome experienced different rates of synonymous or nonsynonymous mutation, and if the rates also depended on the evolutionary history of the population. For synonymous mutations, the rate of mutation was different across functional gene categories ($p < .001$) with no significant effect due to evolutionary history ($p = .89$) nor the interaction between functional category and history ($p = .73$). Pairwise comparisons indicated that the rate of synonymous mutation was significantly higher in the structural gene category ($p < .001$). For nonsynonymous mutations, the rate of mutation was again different across functional categories ($p < .001$) with no significant effect due to history ($p = .62$) nor the interaction of history and functional category ($p = .94$). Pairwise comparisons indicated that the rate of nonsynonymous mutation was significantly higher in the structural gene category ($p < .01$). If we assume that synonymous mutations are neutral, and thus escape the effects of selection, then the signature of elevated synonymous mutation in structural genes must be accounted for by an alternative phenomenon. One possible explanation is the presence of mutation bias (i.e., intrinsic bias in the introduction of genetic variation).

The presence of transition:transversion mutational bias has been documented in experimental microbial populations, with sequence comparisons yielding estimates that are typically 2- to 4-fold greater than null expectations (Stoltzfus & McCandlish, 2017). In this study, the transition:transversion ratio was 1.2 for paths (2-fold higher than expected) and 1.4 for events (3-fold higher). A Pearson's chi-square test was performed to determine whether our observed transition:transversion ratio was different from the null expectation; the test indicated that the observed and expected transition:transversion ratios were significantly different ($\chi^2 = 53.5$; $p < .001$; see "Materials and Methods" for model details).

ON THE POSSIBLE PRESENCE OF RECOMBINATION IN THE EVOLVED POPULATIONS

Previous work in *Saccharomyces cerevisiae* indicates that sex alters molecular signatures of adaptation (McDonald, Rice, & Desai, 2016). In asexual populations, synonymous, nonsynonymous, and intergenic mutations are equally likely to fix because selection cannot efficiently distinguish between their effects due to hitchhiking. In contrast, selection is more efficient in sexual populations, which results in fewer fixed mutations with the overwhelming

majority being nonsynonymous (McDonald et al., 2016). We observed that only 12% of mutations reached fixation, and of those fixed mutations, 91% were nonsynonymous. This is suggestive of recombination; however, further work is required to investigate the contribution of genetic exchange during niche breadth evolution (e.g., analysis of linkage disequilibrium). For example, time-sampled sequencing and analysis of linkage disequilibrium would provide a better understanding of the dynamics of molecular evolution, along with a quantitative assessment of recombination during niche breadth evolution.

APPENDIX B

Appendix B contains two independent tables that can each be found on Figshare:

Appendix Table 1a and 1b
https://doi.org/10.6084/m9.figshare.10010537.v1
Appendix Table 2a and 2b
https://doi.org/10.6084/m9.figshare.10010540.v1